UDC 519.21:004.94:629.735.05 **doi: 10.32620/reks.2025.4.03**

Yevhenii KANARSKYI[1], Vyacheslav KHARCHENKO[1], Oleksandr OREKHOV[1], Yuriy PONOCHOVNYY[2]

[1] ***National Aerospace University "Kharkiv Aviation Institute", Kharkiv, Ukraine***
[2] ***Poltava State Agrarian University, Poltava, Ukraine***

MARKOV MODELLING OF HUMAN-MACHINE INTERACTION IN AN AUGMENTED REALITY ENVIRONMENT FOR UAV/UGV-BASED HAZARDOUS AREA MONITORING SYSTEMS

*The **subject** of the study is Markov processes used for the formal description of the dynamics of states of unmanned vehicles controlled by an operator through augmented reality–based human–machine interfaces. Within the scope of the research, unmanned aerial and ground vehicles are considered as complex multi-state technical systems whose functioning is determined both by their technical characteristics and by the specific features of human interaction with the control interface. The **aim** of the study is to assess the impact of augmented reality–based human–machine interaction interfaces on the error-free decision-making of unmanned system operators, as well as on their responsiveness during control and reaction to changes in system states. The **objectives** of this study are to develop Markov models for the following scenarios: (a) without considering system failures and operator errors, with full recovery; (b) without considering failures, but allowing for operator errors, with full recovery; (c) considering system failures without operator errors, with full recovery; (d) considering both system failures and operator errors, with full recovery; and (e) without considering failures, allowing for operator errors, with the presence of a redundant unmanned system. The resulting Markov chains are intended to be used for modelling and subsequent comparison of the impact of different operating conditions on the system. As a **result** of the study, the following were obtained: (a) a classifier of states of unmanned aerial vehicles within a hazardous environment monitoring system based on the possible presence of failures, operator errors, and system redundancy; (b) Markov models for various system operation scenarios; and (c) simulation results of system operation based on the developed Markov models. **Conclusion**. The scientific novelty is as follows: a method for assessing the availability of monitoring systems with augmented reality–based human–machine interaction interfaces is proposed, which is based on single- and multi-fragment Markov models that take into account operator actions, partial failures, and the availability of reserve unmanned aerial vehicles. The proposed method quantitatively evaluates the impact of augmented reality not only on subjective indicators but also on the overall system availability and reliability indicators.*

Keywords: *augmented reality; unmanned aerial vehicles; Markov chains; human-machine interaction.*

1. Introduction

1.1. Motivation

Monitoring hazardous and potentially hazardous areas to detect explosive ordnance is often one of the most time-consuming tasks due to the high accuracy requirements for the data obtained. Accelerating the execution of such tasks is possible through the use of modern technologies, including cloud computing, digital twins, artificial intelligence (AI), unmanned aerial vehicles (UAVs), unmanned ground vehicles (UGVs), and augmented reality (AR).

Unmanned systems enable the execution of terrain reconnaissance tasks to detect the presence of explosive or other potentially hazardous items. Their high mobility and speed of movement allow access to the most hard-to-reach areas. A suite of sensors, which may include optical detection devices, infrared or multispectral cameras, magnetometers, ground-penetrating radar, and LiDAR, provides the information necessary for subsequent analysis [1].

The information obtained from UAVs and UGVs can be used for analysis by artificial intelligence tools and for creating a digital map of the surveyed area. The application of AI will reduce data analysis time and increase accuracy in the process of detecting potentially explosive items by eliminating the human factor [2]. The use of digital twins in the detection process will allow for the highly accurate identification of unexploded ordnance (UXO), which should reduce the search area for the demining team and increase mission availability levels [3].

The use of cloud technologies for processing and analyzing information provides the necessary level of computational power. Storing and visualizing data in

ISSN 1814-4225 (print)
ISSN 2663-2012 (online)

real time ensures that all participants in the UXO monitoring process have up-to-date information on potential danger zones.

The role of AR in the monitoring process may not be obvious; however, it is precisely human-machine interaction systems based on augmented reality that have the potential to significantly improve the quality of use and the response speed of personnel involved in the monitoring process [4], particularly UAV/UGV operators. An AR interface is capable of providing a high level of operator situational awareness through the simultaneous visualization of current operational parameters of unmanned vehicles, high-resolution video streams, and area maps with plotted mission routes. Determining the impact level of augmented reality interfaces on the reactivity and error-free decision-making of unmanned systems operators during mission execution is one of the most pressing scientific tasks and can be used in the process of assessing their quality.

1.2. State of the art

Over recent decades, research in the field of unmanned monitoring systems has developed along several interconnected directions. The first key research direction focuses on the development of architectures for monitoring systems based on unmanned platforms, including solutions based on UAVs, UGVs, and hybrid UAV/UGV systems, with an emphasis on scalability, reliability, and integration of multi-sensor payloads. The second direction is related to the application of augmented reality technologies to improve human-machine interaction, particularly by enhancing operator situational awareness, reducing cognitive load, and increasing the accuracy and speed of response during interaction with individual unmanned vehicles or their groups. Significant attention here is given to research on the quality of AR interfaces themselves, including their ergonomic characteristics, methods of information presentation, level of immersion, and impact on the accuracy and speed of operator decision-making. Finally, a separate but closely related research direction concerns the modelling and analysis of such systems, including the use of probabilistic and stochastic models to describe system dynamics, operator behaviour, error propagation, and system reliability. In the presented review, existing research in these directions is analysed, their limitations are identified, and unresolved issues motivating the research presented in this work are highlighted.

The first research direction focuses on developing architectures for unmanned vehicle-based monitoring systems, including UAV-only solutions, UGV-based systems, and mixed UAV/UGV configurations.

For example, article [5] examines the use of UAVs as part of an Advanced Air Mobility (AAM) system for autonomous surveillance in smart cities and other tasks, including environmental monitoring. The proposed system is a multi-tiered structure combining a UAV fleet, ground control centres, and edge/cloud computing. Unlike many publications primarily focused on sensor network integration, this work also pays significant attention to reliability and survivability models, which are critically important for monitoring critical infrastructure objects. This approach reflects the trend of transitioning from conceptual to engineering-validated systems capable of functioning under conditions of failures, overloads, and uncertainty.

Another work [6] is dedicated to the use of unmanned systems in the processes of detecting and identifying unexploded ordnance (UXO). Traditionally, performing detection and identification tasks for explosive items relies on using ground robots, ground-penetrating radars, magnetometers, and visual sensors; however, these often suffer from limited adaptability. In this case, the proposed solution addresses this problem through the use of robotic-biological systems that combine technical platforms with biological components. This enhances detection accuracy, reduces risks to personnel, and ensures scalability of solutions for humanitarian demining and security operations. For us, this work is interesting from the perspective of its approach to defining the overall system architecture and the interaction between components.

Work [7] describes the use of UAVs in environmental monitoring systems. The provided review indicates that UAVs are typically equipped with multi-sensor arrays and other measurement modules to ensure the high data quality required for real-time decision-making. Significant attention is also given here to the integration of artificial intelligence methods and automatic flight control. Overall, the work does not contain advanced mission planning algorithms or descriptions of monitoring system architectures, but it demonstrates practical engineering solutions for integrating multi-sensor modules on UAVs, which is relevant for environmental monitoring systems or hazardous areas.

Thus, the reviewed works provide a general understanding of the structure of monitoring systems, the role of unmanned vehicles with multi-sensor modules, and the use of artificial intelligence and cloud computing tools.

At the same time, existing works still have a number of common shortcomings that need to be considered. The first such shortcoming is the insufficient coverage of human-machine interaction mechanisms, their potential impact on the operator and system dynamics, and the possibilities of using modern interfaces, particularly augmented reality, to enhance situational awareness when managing a UAV fleet. The second short-

coming can be noted as the primary focus in the reviewed works being predominantly on the concept and general system structure, whereas the interaction between components, as well as the operator's role under conditions of errors or partial failures, remain described only at a conceptual level. It is also worth separately noting the simplified implementation of the system architecture without considering a swarm approach in work [7]. Combined with the absence of mechanisms for real-time data processing and analysis using cloud computing, this solution could significantly limit its applicability for complex and critical tasks.

In summary, it can be concluded that existing research does not provide a comprehensive integration of UAV-based monitoring system architectures with modern AR interfaces and formal models of operator and system behaviour. Instead, these issues are partially addressed in works [8-16], which belong to the second research direction, namely the use of augmented reality technologies for human-machine interaction in unmanned systems.

Article [8] discusses the use of virtual environments of augmented and virtual reality in UAV control processes. The authors of the study focus on creating an intuitive human-machine interaction system for controlling and servicing unmanned aerial vehicles, which combines the video stream from the drone with overlaid navigation elements. The developed system is used as a tool for detecting and analysing UAV operator errors during test flights. And although the authors of the study note the positive impact of AR on control accuracy and error minimization in the control process, the article provides no calculations or other evidence to support these conclusions.

Study [9] examines the impact of augmented reality on the situational awareness of the operator during UAV flight control. The authors of the work propose using virtual objects to mark UAV movement routes. Based on the results of the experiment conducted in the study, it is claimed that this approach increases the level of situational awareness and operator efficiency. However, this version of the control interface lacks elements responsible for displaying information about the current state of the UAV. This could negatively impact mission performance in the event of the UAV transitioning to a state of partial or complete failure. This scenario and its impact on the accuracy of the operator's actions are not considered by the authors of this study.

A similar application of AR for UGV control is considered in article [10]. The authors of the work suggest an increase in the level of situational awareness for operators of ground vehicles when remote operators use augmented reality interfaces, including for orientation and route planning in an unfamiliar environment. However, the impact of AR on the operator's responsiveness and the accuracy of their actions is not considered, and the assumptions described above lack scientific substantiation.

The authors of [11] reach conclusions regarding the impact of AR on the error-free performance of unmanned system operators that are contrary to those of previous studies. Their research uses an augmented reality interface they developed to assess task performance accuracy and cognitive load levels. The authors also note the low level of situational awareness among the respondents who participated in the study, as well as the low quality of use. It is quite likely that the latter indicator is the reason for the respondents' negative feedback, as in human-machine interaction systems with a high level of immersion, which includes AR, it is one of the key factors. The quality of using AR interfaces directly affects the physical and mental state of operators, which impacts situational awareness, reactivity, and the accuracy of operator decisions [12, 13]. The authors conclude that further research should be directed towards optimizing interfaces to reduce their negative impact on human-machine interaction.

Specifically, study [14] presents an AR interface for mobile devices that enables the control of a UAV fleet using virtual manipulators implemented on a touch screen. However, a significant drawback of this approach is the operator's need to maintain constant visual contact with the drone to monitor flight direction and ensure a stable connection with the mobile device. This limitation is due to the fact that the window displaying the video stream from the UAV occupies less than 10% of the screen area and is partially obscured by virtual control elements. Given the limited size and resolution of mobile device displays, such a small display area makes it difficult or nearly impossible to effectively perceive video information from the UAV's onboard systems. As a result, this approach to using AR may be acceptable for personal use but does not meet the requirements of monitoring systems.

In the work [15], the application of augmented reality for first-person control of UAVs using AR glasses is proposed. Flight control in this case is carried out using a traditional remote control, while video information from the drone's cameras is displayed as virtual windows. This approach is more convenient from the perspective of controlling a single unit; however, it does not provide the capability to control a fleet of UAVs. Furthermore, this AR interface lacks the informational elements necessary for monitoring the unit's status, such as battery level, altitude, speed, etc. Given this, the use of such a solution in monitoring systems is impossible.

In the study [16], a UAV control interface is proposed, which is positioned as a system with augmented reality elements. Unlike the previous approach, it implements the main informational indicators necessary

ISSN 1814-4225 (print)
ISSN 2663-2012 (online)

for controlling an unmanned unit. However, the interface retains a number of limitations, including the small size of the elements intended for displaying the video stream from the UAV and the flight map, as well as the lack of capability for controlling a group of unmanned units. Additionally, the question of classifying the proposed human-machine interaction system as a class of AR interfaces remains debatable, since all virtual control elements are implemented in two-dimensional space, whereas the classical definition of augmented reality [17] assumes their spatial (three-dimensional) placement. Considering the presented approaches and the identified shortcomings of existing AR interfaces, it is advisable to develop and present our own design variant.

The cited research demonstrates significant interest in enhancing operator situational awareness and improving human-machine interaction. However, from the perspective of studying the impact of AR on operator effectiveness within complex monitoring systems, they have a number of fundamental limitations. In particular, the reviewed works focus primarily on the development of individual AR interfaces or experimental prototypes and are generally limited to qualitative or experimental evaluation with small samples, lacking formal modelling of operator and system behaviour over time. In these studies, AR is considered as a visualisation tool, but there is no analysis of how the use of AR affects the probabilities of the system being in various states, the occurrence of errors, or failures. Furthermore, in most works, AR is considered in the context of controlling a single device or a specific task, without accounting for UAV fleets, multi-level management architectures, and partial failure scenarios, which are critical for monitoring systems in hazardous areas. It is also important that none of the reviewed works propose a probability or Markov chain approach to assessing the impact of AR interfaces on operator behaviour and overall system dynamics.

Works focused on the application of Markov models for analysing user and operator behaviour, particularly in augmented reality and unmanned system control, have a number of limitations. For example, in study [18], Markov chains are used to analyse the processing of visual stimuli in 2D, 3D and AR environments as part of a laboratory experiment, which allows conclusions to be drawn about the mechanisms of perception. however, the results obtained are not related to real scenarios of human-machine interaction in complex technical systems, in particular with UAV control or monitoring tasks, where time constraints and the risk of operator errors are critical. In [19], a formalisation of a UAV swarm is proposed in the form of a multi-station queuing system with degradation, but the behaviour of the operator is considered only indirectly and is not linked to interaction interfaces or the use of AR technologies, which limits the ability to assess the impact of humans on the operation of the system. Research [20], which uses hidden Markov models to identify the behavioural patterns of UAV operators, demonstrates the potential of statistical analysis of user actions, but does not take into account the specifics of augmented reality, in particular the spatial placement of information, cognitive load and changes in operator reactivity in AR interfaces.

Taken together, these works confirm the feasibility of using Markov models to describe user behaviour and the states of technical systems, but do not provide a comprehensive approach to modelling the interaction between the operator and the UAV in augmented reality, which justifies the need for further research aimed at combining AR interfaces, formal Markov models and monitoring system architectures in a single study.

1.3. Objectives and methodology

The aim of this work is to develop and analyse a UAV-based hazardous area monitoring system with augmented reality interfaces and to formalise the influence of operator behaviour, human errors, and technical failures on system dynamics using Markov state models. Special attention is given to evaluating the role of AR interfaces in improving situational awareness, operator reactivity, and error-free decision-making.

To achieve this aim, the study analyses existing UAV-based monitoring architectures and their human–machine interaction limitations, develops a generalised system architecture incorporating UAVs/UGVs and an operator AR interface, formalises system and operator behaviour as state-transition models, constructs Markov models for different operational scenarios, performs simulation-based probabilistic analysis of system states, and evaluates the impact of AR interfaces and operator behaviour on overall system performance.

The research methodology combines information system architecture design, Markov process modelling, and simulation techniques. Several system architectures were considered, and the most suitable one was selected for further study. Key factors such as system failures, operator errors, and the availability of backup UAVs/UGVs were classified to define operational scenarios. Five representative scenarios were analysed, covering combinations of failures, operator errors, and reserve systems. For each scenario, an appropriate Markov model was developed, parameterised, and expressed using Kolmogorov–Chapman equations, which were then used for simulation and visualisation of state probabilities.

The article is structured as follows:

- development of a monitoring system architecture (section 2.1);

- development of a availability model classifier based on possible system usage scenarios (section 2.2);

- development and simulation of a system availability models: without accounting for failures and operator errors, with full recovery (section 3.1);

without accounting for failures but with the possibility of operator errors, with full recovery (section 3.2); accounting for failures but without unmanned systems operator errors, with full recovery (section 3.3); accounting for failures and operator errors, with full recovery (section 3.4); without accounting for failures but with the possibility of operator errors, with a reserve unmanned system present (section 3.5);

- discussion of the obtained results (section 4), main contribution. and further research steps (section 5).

2. UAV/UGV-based monitoring system

2.1 System architecture

Since the human-machine interface of augmented reality cannot exist as an object separate from the system, the authors of the study, based on previously reviewed works [1-3], developed a UXO monitoring system architecture that formalises the interrelationships between its functional and informational components. The system is designed for the remote detection, analysis, and spatial localisation of explosive ordnance with minimised risks to personnel.

The scheme presented in Fig. 1 illustrates a comprehensive UXO monitoring system that combines modern technologies for managing unmanned aerial vehicles, augmented reality, as well as centralised data analysis and processing infrastructure. This system ensures efficient, safe, and scalable execution of demining operations, significantly reducing the risk to sappers and enabling work to be conducted in complex and hazardous conditions.

The system's key elements for monitoring system are UAVs and UGVs, which enable remote surveying of hazardous zones, reduce risks for sappers, and provide high-precision data.

UGVs are equipped with optical cameras, thermal and multispectral sensors, magnetometers, and ground-penetrating radar. Combined with AI algorithms and automated processing, these tools identify explosive objects and generate spatial maps of contaminated areas for demining planning.

A central server aggregates and stores critical information—coordinates of hazardous zones, mine threat history, cleared territory maps, telemetry, and video data—and transmits it in real time to the control centre and control station.

The control centre serves as the analytical hub, managing operations, monitoring UAV swarms and demining groups, analysing incoming data, logging events, generating reports, and ensuring information security.

Demining or rescue groups operate directly in the field. Though AR glasses can enhance situational awareness, this study focuses on operator interaction with the monitoring system rather than AR use by deminers (sappers).

The control station, located near the operational area, handles local management, technical support, and UAV/ground system coordination. Operators use remote control units for manual or semi-autonomous control, analyse real-time video, and adjust routes.

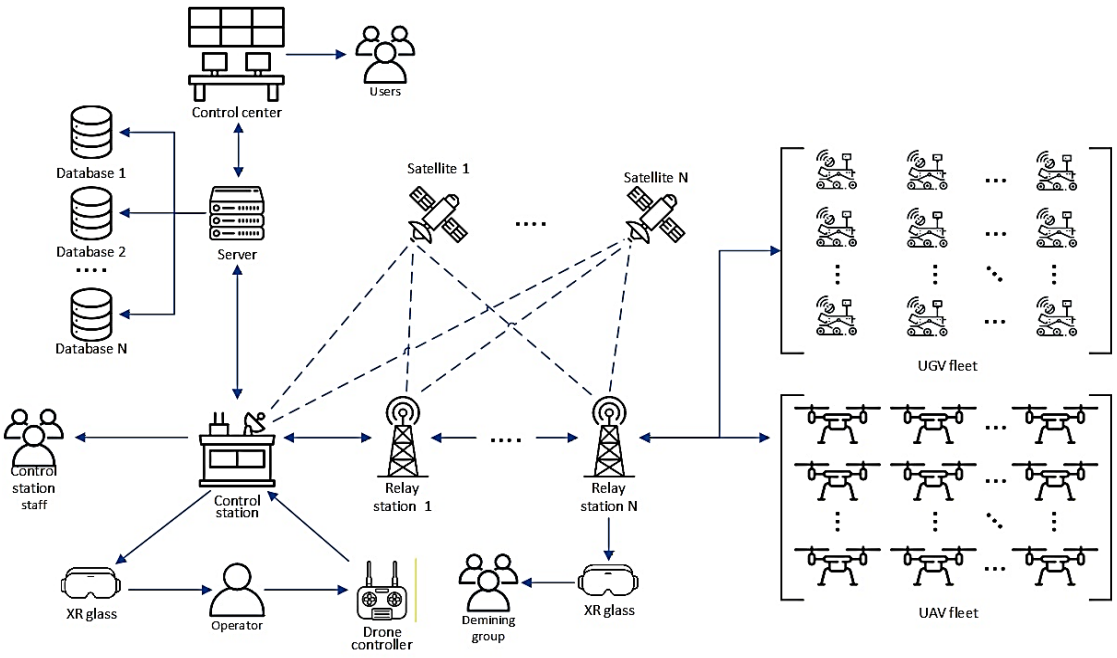

Fig. 1. Architecture of monitoring system

ISSN 1814-4225 (print)
ISSN 2663-2012 (online)

Here, operators employ AR glasses to visualise mine threat maps, UAV and ground system statuses, and telemetry. Their behaviour in AR and transitions between autonomous, semi-autonomous, and manual modes can be formalised with Markov models, enabling quantitative analysis of human-machine interaction.

2.2 Models classification

This work examines several modes in which the monitoring systems UAV may operate considering mission particularities, operator activities, failures and so on.

To systemize various modes and appropriative models and simplify understanding, a multi-level classifier of scenarios (modes) has been developed, covering technical, human and organisational factors that affect the overall system reliability (Fig. 2).

The first level of classification characterises the technical state of the system, determining the presence or absence of failures. The system can operate in normal mode under conditions without malfunctions or transition to states of partial or complete failure when corresponding events are recorded. In the case of combined failures, the scenario of the system transitioning from a state of partial failure to complete failure is considered.

The second level takes into account the possibility of operator errors arising during mission execution. In the case of error-free operator work, the system maintains predictable behaviour, whereas the occurrence of an error causes a transition to one of the subtypes of violations, such as incorrect transition to protected mode, control error, or their combination.

The third level of classification determines the presence of reserve unmanned vehicles and the possibility of restoring operational capability. If reserve drones are present, the option of their replacement until functionality is restored is considered. In the case of no reserves, scenarios are limited to possible partial or complete recovery of the used vehicles.

Base to this classification, several descriptions can be created. In this study, we develop and investigate five models M0-M4. The simplest scenario M0 (red line) considers the case where there are no failures and no operator errors, with full recovery should the system transition into a protected operating mode.

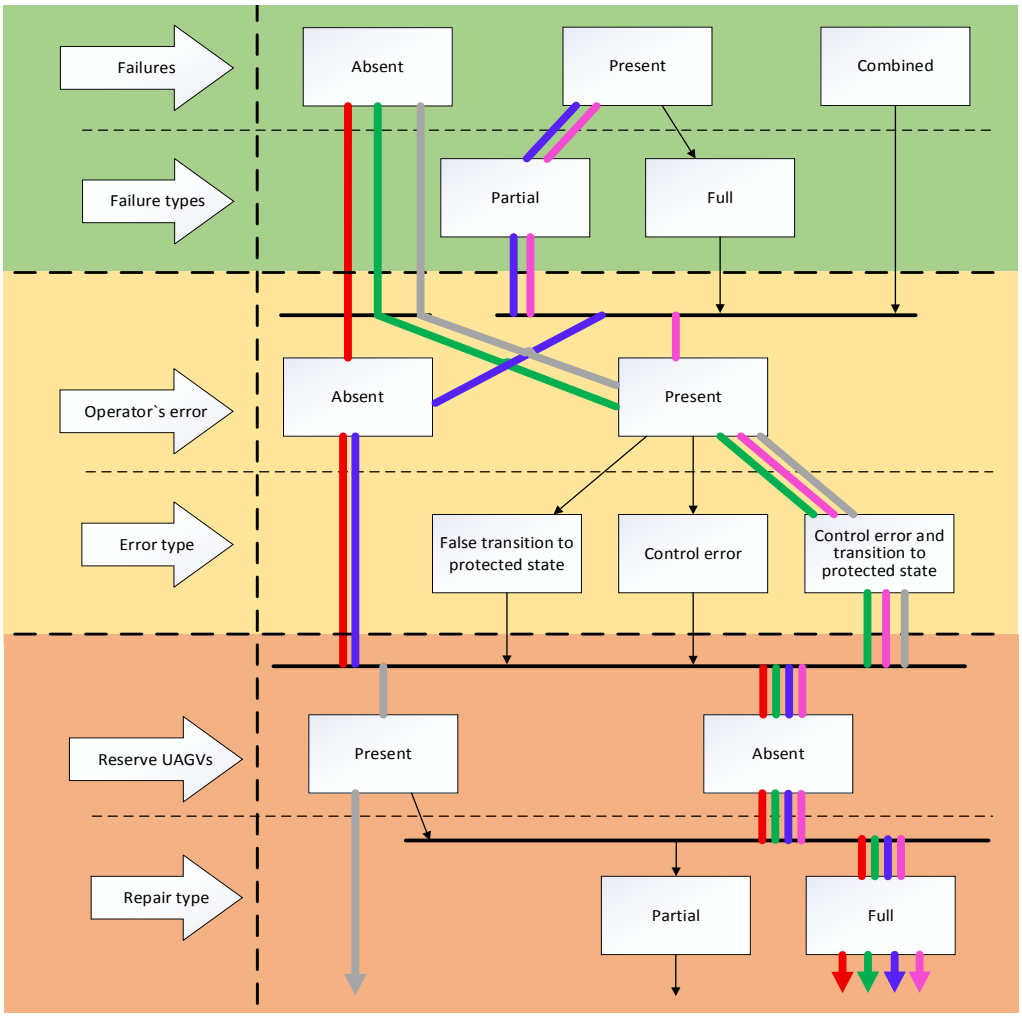

Fig. 2. Models' classification: M0 – red, M1 – green, M2 – blue, M3 – purple, M4 – grey

The first model M1 (green line) considers the case without failures, but with operator errors and full recovery when the system transitions into a protected operating mode.

The second model M2 (blue line) considers a model variant accounting for the presence of faultless operator failures, with full recovery.

The third model M3 (purple line) considers a scenario accounting for failures and operator errors, with full recovery in the event of transitioning to a protected state.

The fourth model M4 (grey line) considers the case without accounting for system failures, with the possibility of operator error, and with the presence of backup UAVs/UGVs.

Thus, the proposed classifier provides a comprehensive representation of possible states of unmanned systems. This approach allows for the formation of formal models, risk assessment in UAV/UGV fleets, prediction of error consequences, and determination of optimal recovery strategies. The obtained structure forms the basis for building analytical and simulation models aimed at improving the availability of unmanned complexes.

3. Markov models

3.1. Initial model, M0

The system described in this paper is characterized by a clearly defined finite set of states between which stochastic transitions occur. At any given time, the system occupies exactly one state, and all possible transitions between states can be described by the corresponding transition intensities. The probability of the system transitioning to a subsequent state depends exclusively on its current state and not on the sequence of preceding transitions. This property is typical of processes in which changes in operating modes are caused by local events (such as operator intervention, erroneous actions, or component failures) and is consistent with the actual logic of operation of monitoring systems as well as with the defining properties of continuous-time Markov processes. Therefore, the use of this classical mathematical framework is both feasible and justified, as it enables the step-by-step development and analysis of monitoring system models.

The simplest case considers a scenario with no failures and no UAV/UGV operator errors, with full recovery if the system enters a protected mode of operation. In this case, the system has only four possible states, as shown on the transition graph of this model (Fig. 3).

System state S_A assumes that the system is in a normal operational state and is controlled by automated means.

System state S_M assumes that the system is in a normal operational state and is manually controlled by the operator.

System state HI_M describes the operator's reaction to the information received during manual control of the system.

System state S_P assumes that the system is in a non-operational, protected state. A forced return is initiated.

To calculate the probabilities of the system being in each of these states, it is necessary to formulate and solve a system of balance equations (1). This system describes the temporal evolution of state probabilities as a function of the transition intensities between states and provides a formal basis for analysing both transient and steady-state behaviour of the monitoring system under autonomous and operator-assisted control modes.

$$\begin{cases} \dfrac{dP_A(t)}{dt} = -(\lambda_{AM} + \lambda_{AP})P_A(t) + \mu_{PA}P_P(t) + \lambda_{MA}P_M(t), \\ \dfrac{dP_M(t)}{dt} = -(\lambda_{MA} + \lambda_{MH} + \lambda_{MP})P_M(t) + \lambda_{AM}P_A(t) + \mu_{HMM}P_{HIM}(t), \\ \dfrac{dP_P(t)}{dt} = -\mu_{PA}P_P(t) + \lambda_{AP}P_A(t) + \lambda_{MP}P_M(t) + \mu_{HMP}P_{HIM}(t), \\ \dfrac{dP_{HIM}(t)}{dt} = -(\mu_{HMP} + \mu_{HMM})P_{HIM}(t) + \lambda_{MH}P_M(t)=0, \\ P_A(t) + P_M(t) + P_P(t) + P_{HIM}(t) = 1, \end{cases} \quad (1)$$

ISSN 1814-4225 (print)
ISSN 2663-2012 (online)

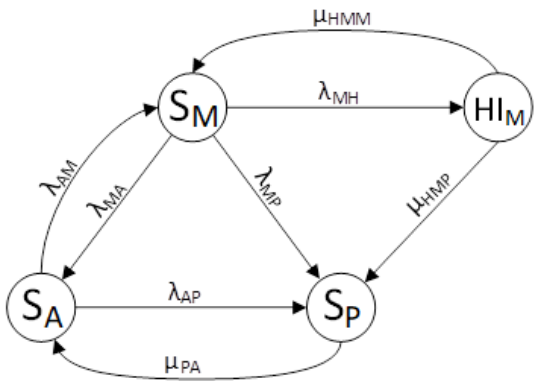

Fig. 3. Transition graph for the model M0

where λ_{AM} – transition intensity from state S_A to state S_M;

λ_{AP} – transition intensity from state S_A to state S_P;

λ_{MA} – transition intensity from state S_M to state S_A;

λ_{MP} – transition intensity from state S_M to state S_P;

λ_{MH} – transition intensity from state S_M to state HI_M;

μ_{PA} – transition intensity from state S_P to state S_A;

μ_{HMM} – transition intensity from state HI_M to state S_M;

μ_{HMP} – transition intensity from state HI_M to state S_P;

P_i – probability of the system being in a state i;

$i \in \{A, M, P, HI_M, F_M, F_{MR}\}$.

For t = 0: $P_A(0) = 1$, $P_M(0) = P_P(0) = P_{HIM}(0) = 0$. Based on the analysis of publications [21–24] devoted to the modelling of systems followed by the assessment of their reliability and availability using Markov processes, the transition parameters were selected for the subsequent simulation of models M0–M4. The transition parameters used in the M0 are summarised in Table 1. These parameters represent the intensities of transitions between system states and are defined in units of hours (hr), which is consistent with the continuous-time Markov chain formulation adopted in this study. The selected parameter ranges reflect realistic operational conditions of UAV/UGV-based monitoring systems and are chosen to capture typical dynamics of autonomous operation, operator intervention, and protective system responses.

Figure 4 presents the time-dependent probabilities of the system being in each operational state, obtained via numerical simulation of the Markov model using the first set of transition parameters defined in Table 1.

Table 1

Transition parameters for the M0

№	Transition	Transition parameter	Measurement range, hr		
			1	2	3
1	$S_A \rightarrow S_M$	λ_{AM}	1	0,3333	2
2	$S_A \rightarrow S_P$	λ_{AP}	2	5	20
3	$S_M \rightarrow S_A$	λ_{MA}	0,3333	0,1	0,6666
4	$S_M \rightarrow S_P$	λ_{MP}	2	5	20
5	$S_M \rightarrow HI_M$	λ_{MH}	0,0083		
6	$S_P \rightarrow S_A$	μ_{PA}	0,5	1	2
7	$HI_M \rightarrow S_M$	μ_{HMM}	0,0008	0,0028	0,0083
8	$HI_M \rightarrow S_P$	μ_{HMP}	2	5	20

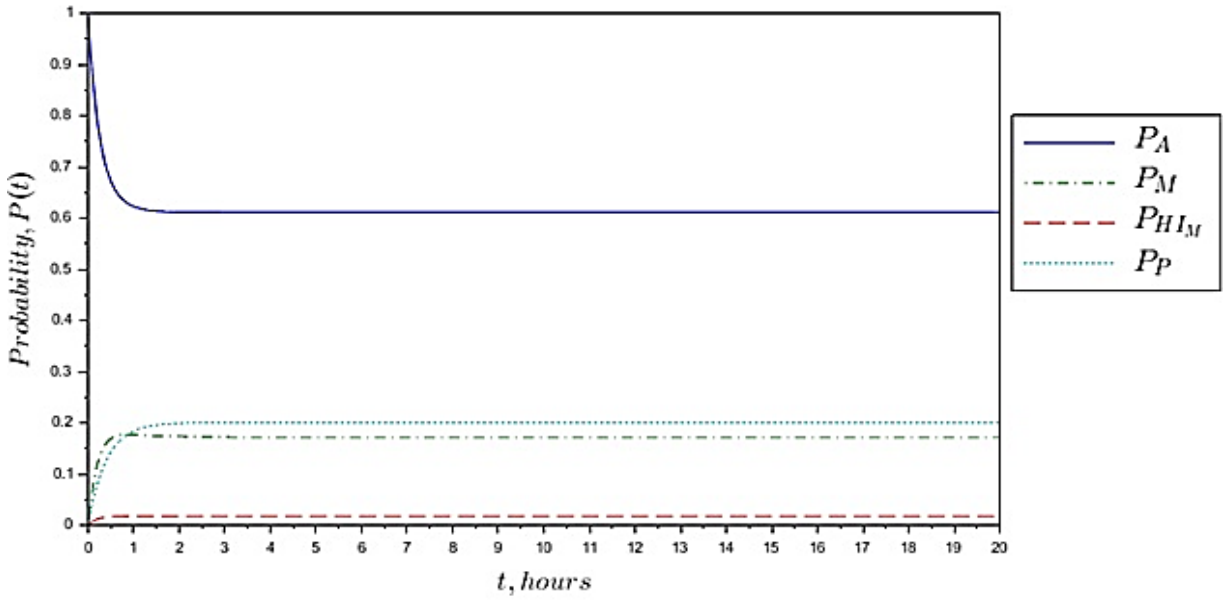

Fig. 4. Simulation results for the M0

The choice of time scale in Fig. 4 and subsequent simulation results is due to the need to investigate the non-stationary part of the behaviour and determine the limits of the system's transition to a steady state, where the probabilities of being in the corresponding states remain unchanged.

Analysis of the graph shows that, for the given transition intensities, the state of normal autonomous operation S_A remains dominant over the entire simulation interval. This indicates that, in the absence of external disturbances or critical failures, the system predominantly operates in autonomous mode, which is both expected and desirable for hazardous area monitoring systems.

The probability of the protected state S_P exhibits an inverse correlation with the probability of autonomous operation S_A: as the likelihood of autonomous functioning decreases, the probability of entering the protected state increases, reflecting the timely activation of safety mechanisms under deteriorating operating conditions.

The probability of the system operating in the manual control state S_M does not exceed $P_M \approx 0.17$ at any time, confirming that manual control serves an auxiliary role and is engaged only in specific situations rather than as a primary operating mode.

The operator response state HI_M maintains a low and nearly constant probability of approximately 0.016 throughout the simulation period, indicating a negligible impact on the overall system dynamics and confirming that active operator intervention is infrequent and not a determining factor in system operation.

3.2. Model considering human errors, M1

The second model considers a scenario without system failures but explicitly accounts for operator errors, assuming full system recovery after transitioning to the protected mode (Fig. 5). Unlike the first model, it incorporates human-related factors, particularly errors during manual control, which may degrade system operability and trigger protective mechanisms.

To represent these effects, two additional states were introduced: complete system inoperability due to operator error during manual control (F_M) and inoperability followed by transition to the protected mode (F_{MR}).

As a result, the number of possible state transitions increased from eight to thirteen, enabling a more realistic quantitative assessment of the impact of operator reliability on system.

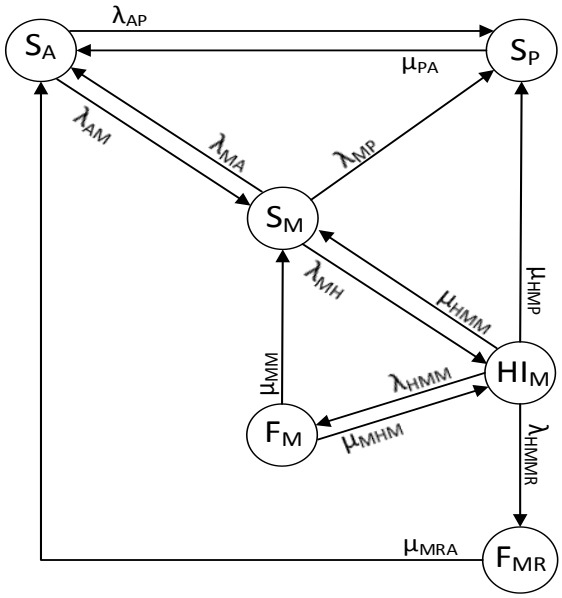

Fig. 5. Transition graph for the model M1

The transition parameters for the M1 are presented in Table 2. Parameters common to the M0 retain their original values and ranges to ensure comparability between the models and to isolate the impact of operator-induced effects.

Table 2

Transition parameters for the M1

№	Transition	Transition parameter	Measurement range, hr		
			1	**2**	**3**
1	$S_A \rightarrow S_M$	λ_{AM}	1	0,3333	2
2	$S_A \rightarrow S_P$	λ_{AP}	2	5	20
3	$S_M \rightarrow S_A$	λ_{MA}	0,3333	0,1	0,6666
4	$S_M \rightarrow S_P$	λ_{MP}	2	5	20
5	$S_M \rightarrow HI_M$	λ_{MH}	0,0083		
6	$S_P \rightarrow S_A$	μ_{PA}	0,5	1	2
7	$HI_M \rightarrow S_M$	μ_{HMM}	0,0008	0,0028	0,0083
8	$HI_M \rightarrow S_P$	μ_{HMP}	2	5	20
9	$HI_M \rightarrow F_M$	λ_{HMM}	5	10	20
10	$HI_M \rightarrow F_{MR}$	λ_{HMMR}	10	100	1000
11	$F_M \rightarrow S_M$	μ_{MM}	0,00016	0,00004	0,00008
12	$F_M \rightarrow HI_M$	μ_{MHM}	0,000128	0,00002	0,0000016
13	$F_{MR} \rightarrow S_A$	μ_{MRA}	0,5	1	2

ISSN 1814-4225 (print)
ISSN 2663-2012 (online)

Additional parameters λ_{HMM} and λ_{HMMR} characterise the intensities of transitions from the operator reaction state HI_M to failure states F_M and F_{MR}, respectively. These parameters are assigned higher values to reflect the increased likelihood of incorrect operator actions under stress or time-critical conditions.

Recovery transitions from failure states (μ_{MM}, μ_{MHM}, μ_{MRA}) are modelled with comparatively low intensities, reflecting the time-consuming nature of diagnosing operator-induced errors and restoring system operability. The relatively higher recovery rate from the protected failure state F_{MR} to autonomous operation S_A assumes that system protection mechanisms facilitate faster stabilisation and recovery.

The chosen parameter ranges enable the evaluation of system robustness under varying degrees of operator reliability and provide a quantitative basis for assessing the impact of human factors on the safety and efficiency of UAV/UGV monitoring systems.

Based on the results of calculations performed using the transition intensities from the first parameter set, the time-dependent probabilities of the system being in each of the possible states were obtained and are presented in Fig. 6. These probabilities characterise the dynamic behaviour of the system under conditions that explicitly take into account operator-related errors.

Compared to the simulation results of the model without operator errors (Fig. 4), the probability of the system operating in the normal autonomous state S_A decreases by approximately 0.03. Despite this reduction, S_A remains the dominant and most probable operating mode throughout the simulation interval, indicating sufficient robustness of the autonomous control mechanisms even in the presence of human-induced disturbances.

The probabilities of the protected state S_P and the manually controlled normal state S_M also slightly decrease; however, these changes are minor and do not qualitatively affect the overall system behaviour. This suggests that the inclusion of operator errors mainly redistributes probabilities among failure-related states rather than significantly influencing the primary operational modes.

Importantly, the probability of the operator response state HI_M remains unchanged compared to the baseline model, indicating that operator reaction frequency is not affected by the introduction of human errors. Instead, the consequences of operator actions become more critical.

A notable result of the M1 is the emergence of a non-negligible probability of system inoperability due to operator error during manual control F_M. Although this probability does not exceed $P_{FM} \approx 0.05$, it is considerably higher than the probability of the operator response state HI_M, highlighting the increased risk associated with manual intervention. In contrast, the probability of inoperability followed by a transition to the protected state F_{MR} remains extremely low and can be neglected within the considered time horizon.

Overall, the results demonstrate that incorporating operator errors enhances the realism by revealing latent risks of manual control while preserving the dominance of autonomous operating modes.

3.3 Model without operator errors and with full recovery, M2

The third case considers a Markov model of the system's operation that accounts for the presence of technical failures in the absence of operator errors and

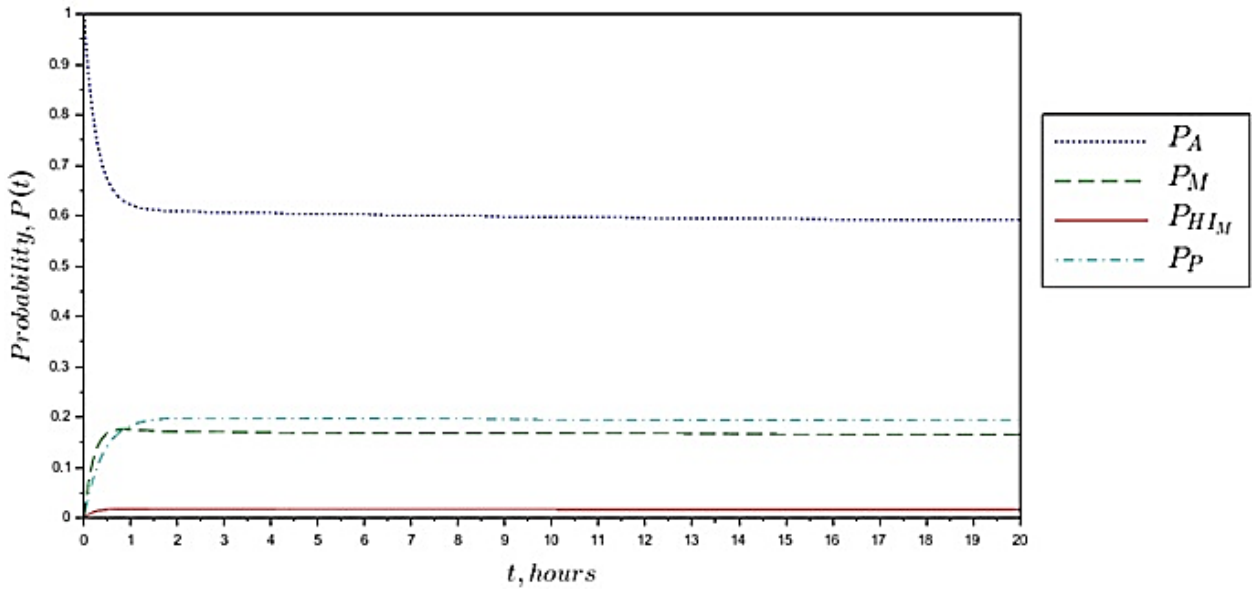

Fig. 6. Simulation for the M1

assumes the possibility of fully restoring the system's functionality. This approach allows for a separate analysis of the impact of hardware and software failures on the system's state dynamics without the additional complication associated with the human factor.

On the transition graph (Fig. 7), the F_M and F_{MR} states are absent, as this scenario does not anticipate operator errors during manual control. Instead, a number of new states have been introduced into the model, reflecting the specifics of partial failures and the system's and operator's response to them. Specifically, the following are considered the manual control state of the system with a partial failure S_{MP}, the operator response state to changes in the system with a partial failure HI_{MP} and the partial operational state of the system due to a partial failure D_L.

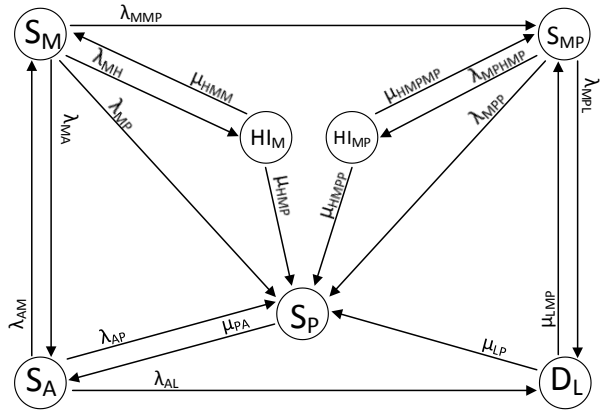

Fig. 7. Transition graph for the model M2

The introduction of these states allows for a more detailed description of the degraded operating modes of the system, which are characteristic of real-world UAV/UGV operations in complex and dynamic environments, as well as for assessing the impact of partial failures on the system's probabilistic characteristics.

The parameters of the transitions for the M2 are provided in Table 3. Each transition parameter characterises the intensity of the system's state change and has a physical interpretation corresponding to the actual operational processes of the monitoring system.

Transitions from autonomous operation S_A to manual control S_M, protected mode S_P, and partial failure D_L are governed by parameters λ_{AM}, λ_{AP}, and λ_{AL}, respectively, with elevated λ_{AL} values reflecting the likelihood of partial technical failures under complex conditions.

Transitions from manual control S_M describe system behaviour under active operator intervention, where λ_{MMP} characterises the risk of transitioning to manual control with partial failure S_{MP}, while λ_{MH} remains low, assuming stable operator behaviour.

Recovery parameters (μ_{PA}, μ_{HMM}, μ_{HMP}, μ_{LMP}, μ_{LP}) represent the system's ability to restore operational capability after failures or interventions.

Special attention is given to partial failure states D_L and S_{MP}, whose mutual transitions model cyclic degradation and recovery processes. The operator response state to partial failures HI_{MP} has extremely low transition intensities, indicating limited operator influence during technical degradation.

Table 3

Transition parameters for the M2

№	Transition	Transition parameter	Measurement range, hr		
			1	2	3
1	$S_A \rightarrow S_M$	λ_{AM}	1	0,3333	2
2	$S_A \rightarrow S_P$	λ_{AP}	2	5	20
3	$S_A \rightarrow D_L$	λ_{AL}	10	25	100
4	$S_M \rightarrow S_A$	λ_{MA}	0,3333	0,1	0,6666
5	$S_M \rightarrow S_P$	λ_{MP}	2	5	20
6	$S_M \rightarrow HI_M$	λ_{MH}	0,0083		
7	$S_M \rightarrow S_{MP}$	λ_{MMP}	10	25	100
8	$S_P \rightarrow S_A$	μ_{PA}	0,5	1	2
9	$HI_M \rightarrow S_M$	μ_{HMM}	0,0008	0,0028	0,0083
10	$HI_M \rightarrow S_P$	μ_{HMP}	2	5	20
11	$D_L \rightarrow S_{MP}$	μ_{LMP}	1	0,3333	2
12	$D_L \rightarrow S_P$	μ_{LP}	2	5	20
13	$S_{MP} \rightarrow D_L$	λ_{MPL}	0,3333	0,1	0,6666
14	$S_{MP} \rightarrow HI_{MP}$	λ_{MPHMP}	0,0083		
15	$S_{MP} \rightarrow S_P$	λ_{MPP}	2	5	20
16	$HI_{MP} \rightarrow S_{MP}$	μ_{HMPMP}	0,0008	0,0028	0,0083
17	$HI_{MP} \rightarrow S_P$	μ_{HMPP}	2	5	20

ISSN 1814-4225 (print)
ISSN 2663-2012 (online)

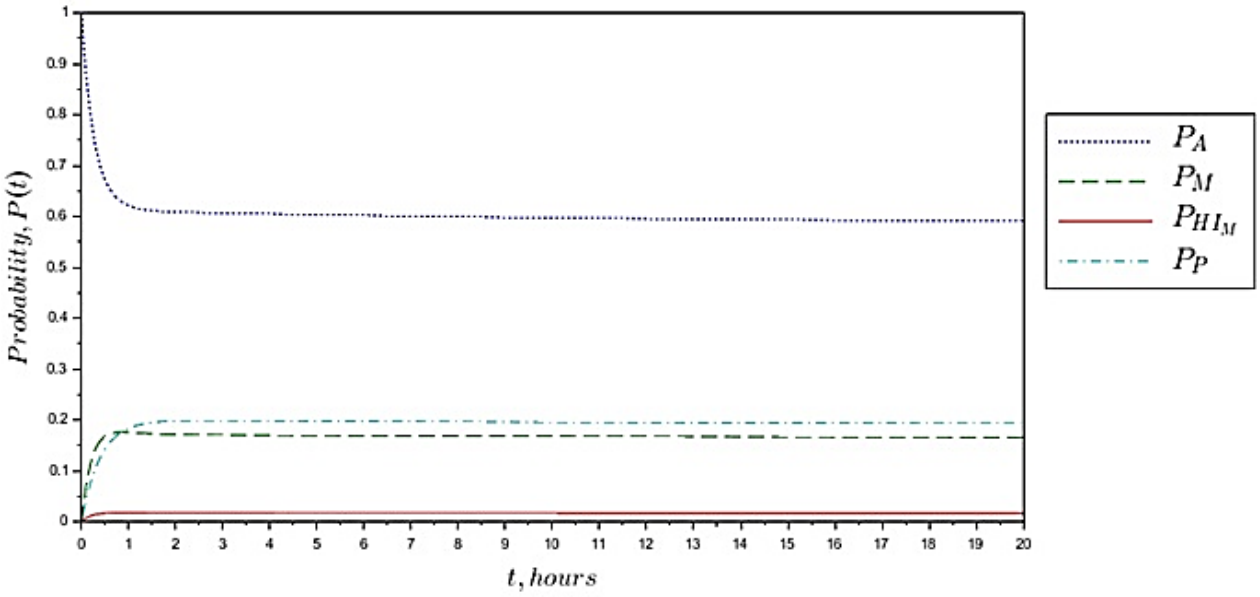

Fig. 8. Simulation for the M2

Parameter ranges are defined for three intensity sets to support sensitivity analysis. Simulation results for the first parameter set show that autonomous operation S_A remains dominant, confirming a high level of system autonomy even in the presence of partial failures.

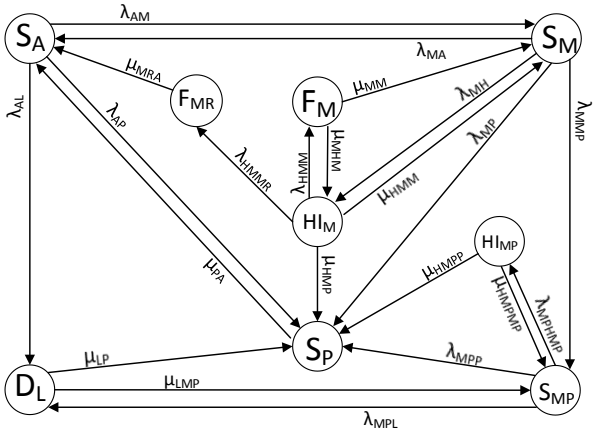

Fig. 9. Transition graph for the model M3

The integration of these specified states and transitions enables the analysis of complex operational scenarios, particularly situations where operator errors can lead to system failures, or conversely, where technical faults prompt operator intervention with an increased risk of erroneous actions. The full restoration of system functionality following a transition to a protected state is modelled as a key mechanism for enhancing the overall reliability and safety of the system's operation.

The transition parameters provided in Table 4 define the transition intensities between the states of the M3, which simultaneously accounts for both system technical failures and operator errors, under the condition of full operational recovery during the transition to a protected mode. The parameter values were selected to ensure consistency with previous models and to reflect the realistic dynamics of the human-machine system's operation under the monitoring of hazardous areas.

The probability of the operator response state HI_M remains almost unchanged compared to previous models, indicating stable operator response characteristics in the absence of erroneous actions. At the same time, an increase in the probability of the protected state S_P and a slight decrease in the probability of the manual control state S_M are observed, which can be attributed to the larger number of failure scenarios that trigger automatic transitions to the protected mode in order to preserve system integrity.

The probability of the manual control state with partial failure S_{MP} is relatively low but nearly twice as high as that of the operator response state HI_M, indicating an increased risk of performance degradation during manual control under partial failure conditions even without operator errors. The probability of the operator response state to partial failures HI_{MP} is extremely low and can be neglected within the scope of this analysis.

A notable probability is associated with the partially operational state D_L, which reaches approximately 0.1. Although this probability does not directly depend on operator intervention, it correlates with a decrease in the probabilities of autonomous operation S_A and manual control S_M, as well as an increase in the probability of

Table 4

Transition parameters for the M3

№	Transition	Transition parameter	Measurement range, hr		
			1	2	3
1	$S_A \rightarrow S_M$	λ_{AM}	1	0,3333	2
2	$S_A \rightarrow S_P$	λ_{AP}	2	5	20
3	$S_A \rightarrow D_L$	λ_{AL}	10	25	100
4	$S_M \rightarrow S_A$	λ_{MA}	0,3333	0,1	0,6666
5	$S_M \rightarrow S_P$	λ_{MP}	2	5	20
6	$S_M \rightarrow HI_M$	λ_{MH}	0,0083		
7	$S_M \rightarrow S_{MP}$	λ_{MMP}	10	25	100
8	$S_P \rightarrow S_A$	μ_{PA}	0,5	1	2
9	$HI_M \rightarrow S_M$	μ_{HMM}	0,0008	0,0028	0,0083
10	$HI_M \rightarrow S_P$	μ_{HMP}	2	5	20
11	$HI_M \rightarrow F_M$	λ_{HMM}	5	10	20
12	$HI_M \rightarrow F_{MR}$	λ_{HMMR}	10	100	1000
13	$F_M \rightarrow S_M$	μ_{MM}	0,05	0,002	0,0001
14	$F_M \rightarrow HI_M$	μ_{MHM}	0,25	0,01	0,08
15	$F_{MR} \rightarrow S_A$	μ_{MRA}	0,5	1	2
16	$D_L \rightarrow S_{MP}$	μ_{LMP}	1	0,3333	2
17	$D_L \rightarrow S_P$	μ_{LP}	2	5	20
18	$S_{MP} \rightarrow D_L$	λ_{MPL}	0,3333	0,1	0,6666
19	$S_{MP} \rightarrow HI_{MP}$	λ_{MPHMP}	0,0083		
20	$S_{MP} \rightarrow S_P$	λ_{MPP}	2	5	20
21	$HI_{MP} \rightarrow S_{MP}$	μ_{HMPMP}	5	10	20
22	$HI_{MP} \rightarrow S_P$	μ_{HMPP}	2	5	20

the S_{MP} state. This indicates that technical degradation alone can lead to partial failures and a reduction in overall system effectiveness, even in the absence of operator errors.

3.4. Model with consideration of operator failures and errors, with full recovery in case of transition to a protected state, M3

This variant considers a Markov model of system operation, which simultaneously accounts for the presence of technical failures and operator errors, and also provides for the full restoration of system functionality in the event of a transition to a protected operating mode. This approach allows the model to approximate the real-world operating conditions of monitoring systems for hazardous areas, where technical malfunctions and human factors may occur simultaneously and mutually influence the overall system dynamics.

In the transition graph (Fig. 9), this model combines the properties of M1 and M2, including all

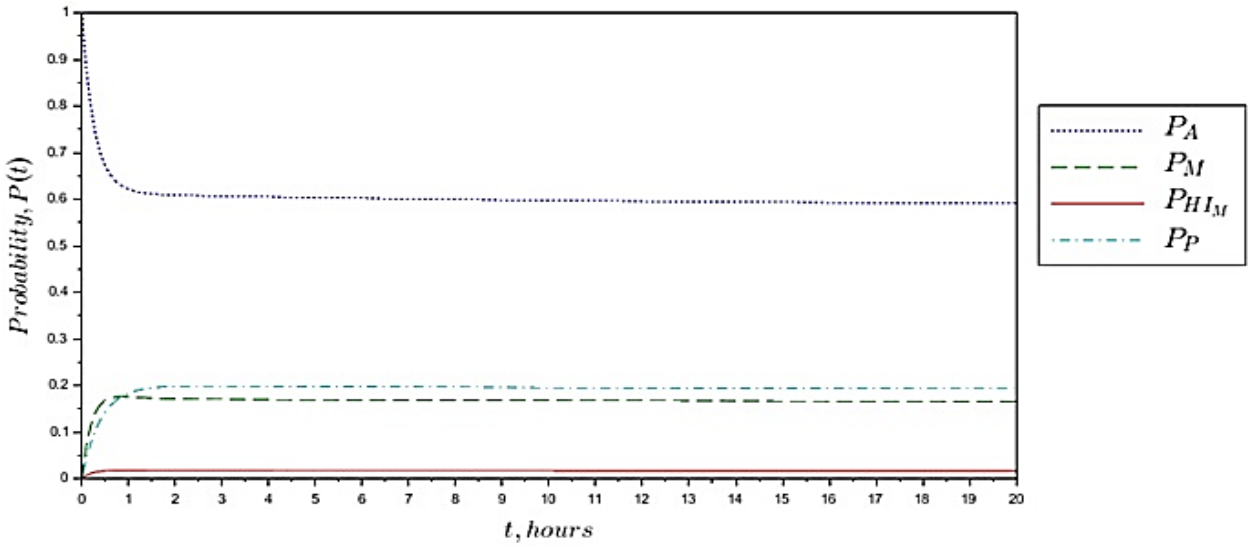

Fig. 10. Simulation for the M3

ISSN 1814-4225 (print)
ISSN 2663-2012 (online)

relevant states associated with autonomous and manual system operation, protected mode, operator response, operator errors, as well as full and partial failures. Thus, the model encompasses both states of non-functionality caused by operator errors (F_M, F_{MR}) and states related to partial technical system failures (D_L, S_{MP}, HI_{MP}), allowing for a comprehensive description of the processes of degradation and recovery of the system's functional capabilities.

Based on the parameter values from the first set of transitions, a model simulation was performed, taking into account the presence of failures and operator errors, with full recovery in the event of a transition to a protected state (Fig. 10).

As in all previous modelling scenarios, the dominant state is normal autonomous operation S_A, confirming stable autonomous functioning even with failures or operator errors. The rapid convergence of S_A probability to a stationary value indicates overall system stability.

The operator response state HI_M remains low and constant, showing limited influence under non-critical conditions. Meanwhile, stable probabilities for the protected state S_P and manual control state S_M reflect the need for operator intervention to handle malfunctions or uncertain conditions, reducing full autonomy.

Manual control with partial failure S_{MP} stays low but consistently higher than HI_M, pointing to increased risks during manual control due to cognitive load or decision-making complexity. Probabilities of operator response to partial failures HI_{MP} and final failures (F_M, F_{MP}) are negligible, confirming effective protective mechanisms.

Degraded operation due to partial failure D_L stabilises around 0.05, with a clear correlation: as S_A decreases, S_M and S_{MP} increase, showing that greater system complexity or operator involvement raises partial failure risks and reduces autonomous performance.

3.5. Two-fragment model, M4

Based on the M1, which describes the system's operation in the absence of failures but accounts for possible operator errors and full restoration of functionality when the system transitions into a protected operating mode, a two-fragment system model was developed. The proposed approach allows the operational process to be divided into interconnected fragments, reflecting the primary and backup control circuits of unmanned systems as described, for example, in study [25].

Unlike previous single-segment models, this version considers a scenario where the system's inherent failures are not taken into account; however, the occurrence of operator errors during manual or semi-autonomous control is permitted. Additionally, the presence of backup unmanned systems is envisaged, which can be engaged in case of reduced effectiveness or erroneous actions by the operator in the primary system fragment. This approach allows for a more accurate simulation of real-world operating conditions of monitoring systems, where the redundancy of technical means is one of the key mechanisms for enhancing reliability and resilience.

A transition graph of the M4, illustrating the interaction between the primary and backup system fragments, as well as the possible transitions between their states, is provided in Fig. 11.

The equation for the two-fragment model is presented in formula (2), which describes the system of Kolmogorov differential equations for the probabilities of the system being in each of the possible states, taking into account the interaction of two interconnected fragments of the model. Initial conditions are the similar to formula (1).

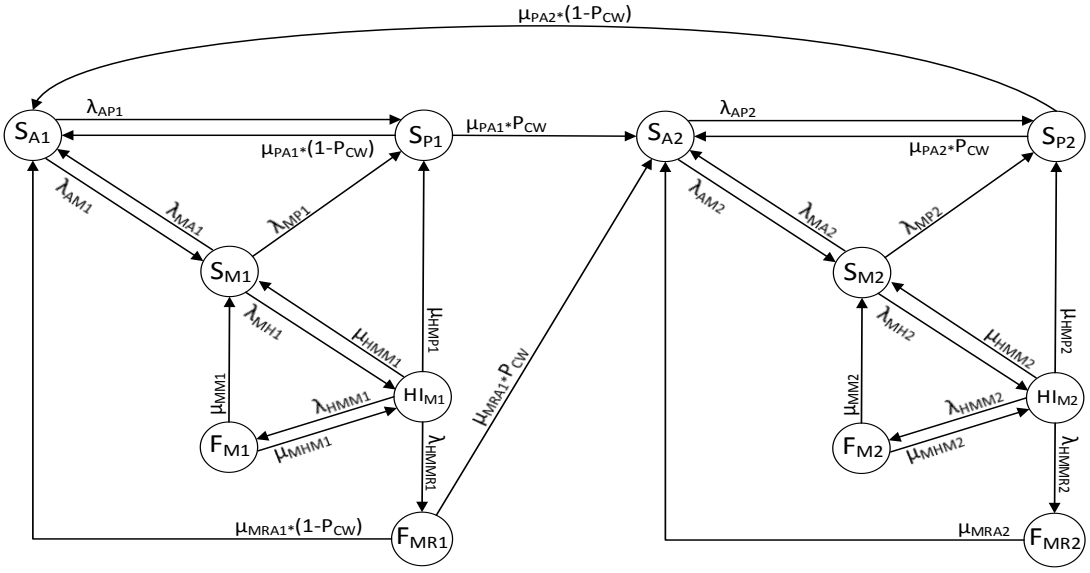

Fig.11. Transition graph for the model M4

$$
\begin{cases}
\frac{dP_{A1}(t)}{dt} = -(\lambda_{AM1}+\lambda_{AP1})P_{A1}(t) + \mu_{PA1}(1-P_{CW})P_{P1}(t) + \lambda_{MA1}P_{M1}(t) + \mu_{MRA1}(1-P_{CW})P_{FMR1}(t) + \mu_{PA2}(1-P_{CW})P_{P2}(t) \\
\frac{dP_{M1}(t)}{dt} = -(\lambda_{MA1}+\lambda_{MP1}+\lambda_{MH1})P_{M1}(t) + \lambda_{AM1}P_{A1}(t) + \mu_{HMM1}P_{HMM1}(t) + \mu_{MM1}P_{FM1}(t) \\
\frac{dP_{P1}(t)}{dt} = -(\mu_{PA1}(1-P_{CW}) + \mu_{PA1}P_{CW})P_{P1}(t) + \lambda_{AP1}P_{A1}(t) + \lambda_{MP1}P_{M1}(t) + \mu_{HMP1}P_{HIM1}(t) \\
\frac{dP_{HIM1}(t)}{dt} = -(\mu_{HMM1} + \mu_{HMP1} + \lambda_{HMM1} + \lambda_{HMMR1})P_{HIM1}(t) + \lambda_{MH1}P_{M1}(t) + \mu_{MHM1}P_{FM1}(t) \\
\frac{dP_{FM1}(t)}{dt} = -(\mu_{MM1} + \mu_{MHM1})P_{FM1}(t) + \lambda_{HMM1}P_{HIM1}(t) \\
\frac{dP_{FMR1}(t)}{dt} = -(\mu_{MRA1}(1-P_{CW}) + \mu_{MRA1}P_{CW})P_{FMR1}(t) + \lambda_{HMMR1}P_{HIM1}(t) \\
\frac{dP_{A2}(t)}{dt} = -(\lambda_{AM2} + \lambda_{AP2})P_{A2}(t) + \mu_{PA2}P_{CW}P_{P1}(t) + \mu_{PA2}P_{P2}(t) + \lambda_{MA2}P_{M2}(t) + \mu_{MRA2}P_{FMR2}(t) + \mu_{MRA1}P_{CW}P_{FMR1}(t) \\
\frac{dP_{M2}(t)}{dt} = -(\lambda_{MA2}+\lambda_{MP2}+\lambda_{MH2})P_{M2}(t) + \lambda_{AM2}P_{A2}(t) + \mu_{HMM2}P_{HMM2}(t) + \mu_{MM2}P_{FM2}(t) \\
\frac{dP_{P2}(t)}{dt} = -(\mu_{PA2}P_{CW} + \mu_{PA2}(1-P_{CW}))P_{P2}(t) + \lambda_{AP2}P_{A2}(t) + \lambda_{MP2}P_{M2}(t) + \mu_{HMP2}P_{HIM2}(t) \\
\frac{dP_{HIM2}(t)}{dt} = -(\mu_{HMM2} + \mu_{HMP2} + \lambda_{HMM2} + \lambda_{HMMR2})P_{HIM2}(t) + \lambda_{MH2}P_{M2}(t) + \mu_{MHM2}P_{FM2}(t) \\
\frac{dP_{FM2}(t)}{dt} = -(\mu_{MM2}+\mu_{MHM2})P_{FM2}(t) + \lambda_{HMM2}P_{HIM2}(t) \\
\frac{dP_{FMR2}(t)}{dt} = -\mu_{MRA2}P_{FMR2}(t) + \lambda_{HMMR2}P_{HIM2}(t) \\
P_{A1}(t) + P_{M1}(t) + P_{P1}(t) + P_{HIM1}(t) + P_{FM1}(t) + P_{FMR1}(t) + P_{A2}(t) + P_{M2}(t) + P_{P2}(t) + P_{HIM2}(t) + P_{FM2}(t) + P_{FMR2}(t)=1
\end{cases}
\tag{2}
$$

where λ_{AMi} – transition intensity from state S_{Ai} to state S_{Mi};

λ_{APi} – transition intensity from state S_{Ai} to state S_{Pi};

λ_{MAi} – transition intensity from state S_{Mi} to state S_{Ai};

λ_{MPi} – transition intensity from state S_{Mi} to state S_{Pi};

λ_{MHi} – transition intensity from state S_{Mi} to state HI_{Mi};

μ_{PAi} – transition intensity from state S_{Pi} to state S_{Ai};

μ_{HMMi} – transition intensity from state HI_{Mi} to state S_{Mi};

μ_{HMPi} – transition intensity from state HI_{Mi} to state S_{Pi};

λ_{HMMi} – transition intensity from state HI_{Mi} to state F_{Mi};

λ_{HMMRi} – transition intensity from state HI_{Mi} to state F_{MRi};

μ_{MMi} – transition intensity from state F_{Mi} to state S_{Mi};

μ_{MHMi} – transition intensity from state F_{Mi} to state HI_{Mi};

μ_{MRAi} – transition intensity from state F_{MRi} to state S_{Ai};

P_{CW} – probability of a successful switch to the reserve fragment;

P_{ji} – probability of the system being in a state j;

$j \in \{A, M, P, HI_M, F_M, F_{MR}\}$, $i \in \{1, 2\}$.

The transition parameters for the M4 are presented in Table 5 and define the transition intensities between states for the main and reserve fragments of the system. The proposed parameter values are based on the assumption of identical functional characteristics of both system fragments, as well as maintaining consistency with parameters used in previous models, which allows for a correct comparative evaluation of simulation results.

Overall, the selected parameter set allows the M4 to be effectively applied for assessing the reliability and resilience of AR-oriented UAV/UGV-based monitoring systems with redundancy. Figure 12 presents the simulation results of M4, illustrating the temporal evolution of state probabilities and enabling analysis of redundancy effectiveness, operator influence, and system stability in the steady-state regime.

The principal feature of the two-fragment model is the introduction of the P_{CW} (Probability of Correct Switching) parameter, which represents the likelihood of a successful switch to the reserve fragment during recovery from the protected state or after failure states F_{MRi}. The P_{CW} value varies from 0.5 to 0.9, reflecting different efficiencies of redundancy management and automatic recovery mechanisms.

ISSN 1814-4225 (print)
ISSN 2663-2012 (online)

Table 5

Transition parameters for the M4

№	Transition	Transition parameter	Measurement range, hr		
			1	2	3
1	$S_{A1} \rightarrow S_{M1}$	λ_{AM1}	1	0,3333	2
2	$S_{A1} \rightarrow S_{P1}$	λ_{AP1}	2	5	20
3	$S_{M1} \rightarrow S_{A1}$	λ_{MA1}	0,3333	0,1	0,6666
4	$S_{M1} \rightarrow S_{P1}$	λ_{MP1}	2	5	20
5	$S_{M1} \rightarrow HI_{M1}$	λ_{MH1}	0,0083		
6	$S_{P1} \rightarrow S_{A1}$	$\mu_{PA1}(1\text{-}P_{CW})$	0,5*(1-P_{CW})	1*(1-P_{CW})	2*(1-P_{CW})
7	$S_{P1} \rightarrow S_{A2}$	$\mu_{PA1}P_{CW}$	0,5*P_{CW}	1*P_{CW}	2* (1-P_{CW})
8	$HI_{M1} \rightarrow S_{M1}$	μ_{HMM1}	0,0008	0,0028	0,0083
9	$HI_{M1} \rightarrow S_{P1}$	μ_{HMP1}	2	5	20
10	$HI_{M1} \rightarrow F_{M1}$	λ_{HMM1}	5	10	20
11	$HI_{M1} \rightarrow F_{MR1}$	λ_{HMMR1}	10	100	1000
12	$F_{M1} \rightarrow S_{M1}$	μ_{MM1}	0,00016	0,00004	0,000008
13	$F_{M1} \rightarrow HI_{M1}$	μ_{MHM1}	0,000128	0,00002	0,0000016
14	$F_{MR1} \rightarrow S_{A1}$	$\mu_{MRA1}(1\text{-}P_{CW})$	0,5*(1-P_{CW})	1*(1-P_{CW})	2*(1-P_{CW})
15	$F_{MR1} \rightarrow S_{A2}$	$\mu_{MRA1}P_{CW}$	0,5*P_{CW}	1*P_{CW}	2* (1-P_{CW})
16	$S_{A2} \rightarrow S_{M2}$	λ_{AM2}	1	0,3333	2
17	$S_{A2} \rightarrow S_{P2}$	λ_{AP2}	2	5	20
18	$S_{M2} \rightarrow S_{A2}$	λ_{MA2}	0,3333	0,1	0,6666
19	$S_{M2} \rightarrow S_{P2}$	λ_{MP2}	2	5	20
20	$S_{M2} \rightarrow HI_{M2}$	λ_{MH2}	0,0083		
21	$S_{P2} \rightarrow S_{A2}$	$\mu_{PA2}P_{CW}$	0,5*P_{CW}	1*P_{CW}	2* (1-P_{CW})
22	$S_{P2} \rightarrow S_{A1}$	$\mu_{PA2}(1\text{-}P_{CW})$	0,5*(1-P_{CW})	1*(1-P_{CW})	2*(1-P_{CW})
23	$HI_{M2} \rightarrow S_{M2}$	μ_{HMM2}	0,0008	0,0028	0,0083
24	$HI_{M2} \rightarrow S_{P2}$	μ_{HMP2}	2	5	20
25	$HI_{M2} \rightarrow F_{M2}$	λ_{HMM2}	5	10	20
26	$HI_{M2} \rightarrow F_{MR2}$	λ_{HMMR2}	10	100	1000
27	$F_{M2} \rightarrow S_{M2}$	μ_{MM2}	0,00016	0,00004	0,000008
28	$F_{M2} \rightarrow HI_{M2}$	μ_{MHM2}	0,000128	0,00002	0,0000016
29	$F_{MR2} \rightarrow S_{A2}$	μ_{MRA2}	0,5	1	2
		P_{CW}	0,5	0,7	0,9

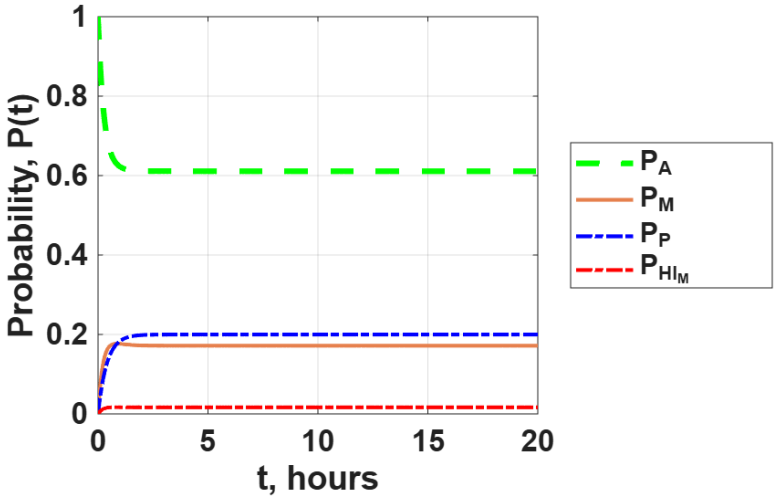

Fig. 12. Simulation for the M4

Transitions such as $S_{P1} \rightarrow S_{A1}$ / S_{A2}, $F_{MR1} \rightarrow S_{A1}$ / S_{A2}, and their counterparts for the second fragment are weighted by the P_{CW} coefficient, thereby modelling the probabilistic distribution between restoring operation of the current fragment and activating the reserve. The share $(1 - P_{CW})$ corresponds to recovery of

the primary fragment, while P_{CW} represents successful switching to the reserve.

Transition parameters from operator response states HI_{Mi} to failure states F_{Mi} and F_{MRi} characterise the probability of operator-induced errors during manual control and are inherited from previous models, reflecting an increased risk of critical errors. Low reverse transition intensities indicate slow recovery and prolonged residence in failure-related states. Identical parameters in both fragments eliminate subsystem asymmetry, allowing the analysis to focus on the effect of redundancy on reliability and mitigation of the human factor.

Compared to the single-fragment model, the M4 shows an increase of approximately 0.05 in the probability of normal autonomous operation S_A, which remains the dominant system state, indicating improved operational stability in the presence of operator influence. Probabilities of the protected state S_P and manual control state S_M also increase slightly, without significantly affecting overall state distribution. The operator response state HI_M remains at levels similar to previous models, indicating minimal impact of the two-fragment structure on operator dynamics.

The probability of system inoperability due to operator error during manual control S_{FM} remains nearly unchanged and does not exceed 0.05 after stabilisation. Its higher value compared to HI_M suggests that operator actions more often lead to errors than successful disturbance compensation. The probability of transition to a protected inoperable state F_{MR} is negligible and can be excluded from further analysis. Overall, the results confirm the suitability of the M4 for analysing the impact of the human factor on system reliability and stability.

4. Results and Discussion

The obtained results show that the probability of the system being in the protected state is directly determined by the control mode, automatic or manual. Analysis of the time-dependent state probabilities reveals a short transient process, after which the system reaches a steady-state regime, with the most intensive probability redistribution occurring at the initial stage of operation.

Throughout the simulation, normal autonomous operation S_A remains the dominant state: its probability decreases from the initial value but stabilises at the highest level, confirming high autonomous stability. An inverse relationship between S_A and the protected state SP is observed, where reduced autonomy leads to an increased protected-state probability, indicating an adequate system response.

The probability of the manual control state S_M increases at the beginning of the simulation, then stabilises and does not exceed 0.17, demonstrating the auxiliary role of manual control. At the same time, the probability of the manual control state with partial failure S_{MP} remains low but exceeds that of the operator response state HI_M, indicating an increased risk of partial failures during manual operation.

The probabilities of operator response to partial failures HI_{MP}, as well as the emergency states F_M and F_{MP}, are extremely small and have a negligible impact on overall system dynamics. In contrast, the probability of the degraded performance state D_L is noticeable and stabilises at approximately 0.05, showing no direct dependence on immediate operator intervention.

The operator response state HI_M maintains a constant probability over time, indicating that operator reactions do not significantly influence steady-state system behaviour. Finally, automatic control reduces the likelihood of transitions to the protected state compared to manual control, reflecting the impact of the human factor. The probabilities of transitions to inoperable states due to operator errors remain low under the considered conditions.

The applicability limits of the proposed models are determined by the types of UAVs, their missions, and the characteristics of the cyber-physical environment, provided that these factors do not violate the formulated assumptions to an extent that would significantly affect the accuracy of the results, in particular the calculation of the availability index. If such an influence becomes critical, it is necessary to employ semi-Markov models or simulation-based modelling.

Despite the fact that this article mainly refers to the use of UAVs, the Markov models obtained describe the states of the system and the transitions between them in such a way that they can be used to model the operation of UGVs.

The impact of hazardous environments can be taken into account through appropriate coefficients that increase the failure rate or the probability of mission abortions. This work does not consider in detail scenarios of such impacts, including cyber-attacks, which may be the subject of further research.

The trustworthiness of the proposed models is confirmed through their theoretical consistency with the properties of Markov processes, including prob-ability normalization and non-negativity of transition intensities. Additional validation is provided by the agreement of the obtained results with known limit-ing cases and trends reported in related studies on Markov-based reliability and availability modelling. Furthermore, a numerical stability and sensitivity analysis demonstrates that moderate variations in the transition parameters do not lead to qualitative changes in the system behaviour, confirming the credibility of the proposed approach.

ISSN 1814-4225 (print)
ISSN 2663-2012 (online)

5. Conclusions

The article substantiates the expediency of using Markov chains for formalised modelling of user and system behaviour in augmented reality. This approach represents human-machine interaction as a finite set of states with probabilistic transitions, enabling quantitative analysis of AR-based monitoring and control systems.

The main contribution is the study of UAV monitoring systems where AR serves as a key element of interaction. Unlike most works that examine architecture, interfaces, and operator behaviour separately, this research integrates them into one applied task, considering operating modes (autonomous, manual, protected), failures, operator errors, and backup drones.

The scientific novelty lies in a newly proposed method for assessing the availability of monitoring systems for potentially hazardous areas with augmented reality–based human–machine interaction interfaces, which, unlike existing approaches, is based on single- and multi-fragment Markov models and accounts for operator reactivity and error-free performance, partial failures, and the availability of reserve UAVs, thereby enabling analysis of parameter impacts on the readiness function and their justified selection to meet specified requirements.

Simulation results show rapid transition to steady state, with autonomous operation remaining dominant, confirming its stability. An inverse correlation between autonomous and protected states indicates adequate system response to reduced capability. Manual control plays a supporting role but carries higher risk of partial failures, while operator response state has minimal influence.

Thus, the study confirms the feasibility of Markov models for analysing complex AR-integrated systems and provides a basis for modelling other cyber-physical systems, optimising AR interface design, and supporting engineering solutions to enhance reliability, safety, and efficiency of UAV/UGV-based systems.

Contributions of authors: conceptualization, methodology – **Oleksandr Orekhov, Vyacheslav Kharchenko**, formulation of tasks, development and parametrization of models – **Yevhenii Kanarskyi;** preparation and simulation of models, visualization – **Yevhenii Kanarskyi, Yuriy Ponochovnyy;** verification, analysis of results, writing, original draft preparation – **Yevhenii Kanarskyi;** review and editing – **Oleksandr Orekhov, Vyacheslav Kharchenko.**

Conflict of Interest

The authors declare that they have no conflict of interest in relation to this research, whether financial, personal, author ship or otherwise, that could affect the research and its results presented in this paper.

Financing

This study was conducted without financial support.

Data Availability

Data will be made available upon reasonable request.

Use of Artificial Intelligence

The authors confirm that they did not use artificial intelligence technologies when creating the current work.

All the authors have read and agreed to the published version of this manuscript.

References

1. Zatserkovnyi, V., Tsiupa, I., De Donatis, M., Nikoliuk, I., Kravchenia, V., Tsvyk, O., & Mironchuk, T. Methods to detect explosive hazards in agricultural areas. *Visnyk of Taras Shevchenko National University of Kyiv. Geology*, 2025, vol. 3, no. 110, pp. 127-138. DOI: 10.17721/1728-2713.110.14.

2. Hameed, Q. A., Hussein, H. A., Ahmed, M. A., Salih, M. M., Ismael, R. D., & Omar, M. B. UXO-AID: A New UXO Classification Application Based on Augmented Reality to Assist Deminers. *Computers*, 2022, vol. 11, iss. 8, article no. 124. DOI: 10.3390/computers11080124.

3. Blachnik, M., Przyłucki, R., Golak, S., Ściegienka, P., & Wieczorek, T. On the Development of a Digital Twin for Underwater UXO Detection Using Magnetometer-Based Data in Application for the Training Set Generation for Machine Learning Models. *Sensors*, 2023, vol. 23, iss. 15, article no. 6806. DOI: 10.3390/s23156806.

4. Jefry, N. F. S., & Rambli, D. R. A. A review of augmented reality systems and their effects on mental workload and task performance. *Heliyon*, 2021, vol. 7, iss. 3, article no. e06277. DOI: 10.1016/j.heliyon.2021.e06277.

5. Fesenko, H., Illiashenko, O., Kharchenko, V., Kliushnikov, I., Morozova, O., Sachenko, A., & Skorobohatko, S. Flying sensor and edge network-based advanced air mobility systems: reliability analysis and applications for urban monitoring. *Drones*, 2023, vol. 7, iss. 7, article no. 409. DOI: 10.3390/drones7070409.

6. Fedorenko, G., Fesenko, H., Kharchenko, V., Kliushnikov, I., & Tolkunov, I. Robotic-biological systems for detection and identification of explosive ordnance: concept, general structure, and models. *Radioelectronic and Computer Systems*, 2023, no. 2, pp. 143-159. DOI: 10.32620/reks.2023.2.12.

7. Sharma, S., Muley, A., Singh, R., & Gehlot, A. UAV for surveillance and environmental monitoring. *Indian Journal of Science and Technology*, 2016, vol. 9, iss. 43, pp. 1-4. DOI: 10.17485/ijst/2016/v9i43/104396.

8. Misse, E. S., Villacrés, S. A., Velasco, P. M., & Andaluz, V. H. Augmented reality system for the assistance of unmanned aerial vehicles. *15th Iberian Conference on Information Systems and Technologies (CISTI)*, Seville, Spain, IEEE, 2020, pp. 1-6. DOI: 10.23919/CISTI49556.2020.9140958.

9. Ruano, S., Cuevas, C., Gallego, G., & García, N. Augmented reality tool for the situational awareness improvement of UAV operators. *Sensors*, 2017, vol. 17, iss. 2, article no. 297. DOI: 10.3390/s17020297.

10. Mutzenich, C., Durant, S., Helman, S., & Dalton P. Updating our understanding of situation awareness in relation to remote operators of autonomous vehicles. *Cognitive Research: Principles and Implications*, 2021, vol. 6, article no. 9. DOI: 10.1186/s41235-021-00271-8.

11. Kalatzis, A., Prabhu, V. G., Stanley, L., & Wittie, M. P. Effect of augmented reality user interface on task performance, cognitive load, and situational awareness in human–robot collaboration. *32nd IEEE International Conference on Robot and Human Interactive Communication (RO-MAN)*, Busan, Republic of Korea, IEEE, 2023, pp. 1252-1259. DOI: 10.1109/RO-MAN57019.2023.10309468.

12. Seeling, P. Augmented reality device operator cognitive strain determination and prediction. *AIMS Electronics and Electrical Engineering*, 2017, vol. 1, iss. 1, pp. 100-110. DOI: 10.3934/ElectrEng. 2017.1.100.

13. Kaufeld, M., Mundt, M., Forst, S., & Hecht, H. Optical see-through augmented reality can induce severe motion sickness. *Displays*, 2022, vol. 74, article no. 102283. DOI: 10.1016/j.displa.2022.102283.

14. Costa, C., Gomes, E., Rodrigues, N., Gonçalves, A., Ribeiro, R., Costa, P., & Pereira, A. Augmented reality mobile digital twin for unmanned aerial vehicle wildfire prevention. *Virtual Reality*, 2025, vol. 29, article no. 71. DOI: 10.1007/s10055-025-01145-w.

15. Sautenkov, O., Asfaw, S., Yaqoot, Y., Mustafa, M. A., Fedoseev, A., Trinitatova, D., & Tsetserukou, D. FlightAR: AR flight assistance interface with multiple video streams and object detection aimed at immersive drone control. *IEEE International Conference on Robotics and Biomimetics (ROBIO)*, Bangkok, Thailand, IEEE, 2024, pp. 614-619. DOI: 10.1109/ROBIO64047.2024.10907428.

16. Bagassi, S., Fadda, T., & Corsi, M. *Advanced human machine interfaces for drone monitoring: assessment of the technological framework for the design of an augmented reality interface*. Available at: https://www.icas.org/icas_archive/icas2024/data/papers/icas2024_1059_paper.pdf (accessed: 27 September 2025).

17. Azuma, R.T. A survey of augmented reality. *Presence: Teleoperators and Virtual Environments*, 1997, vol. 6, iss. 4, pp. 355-385. DOI: 10.1162/pres.1997.6.4.355.

18. Mugruza-Vassallo, C. A., Granados-Domínguez, J. L., Flores-Benites, V., & Córdova Berríos, L. L. Different Markov chains modulate visual stimuli processing in a Go–Go experiment in 2D, 3D, and augmented reality. *Frontiers in Human Neuroscience*, 2022, vol. 16, pp. 1-13. DOI: 10.3389/fnhum.2022.955534.

19. Kliushnikov, I., Fesenko, H., Fedorenko, G., Rudakov, S., Mikhalevskyi, V., & Kompaniiets, O. Swarm of unmanned aerial vehicles as a multistate queueing system with non-controlled and controlled degradation. *12th International Conference on Dependable Systems, Services and Technologies (DESSERT)*, Athens, Greece, IEEE, 2022, pp. 1-7. DOI: 10.1109/DESSERT58054.2022.10018784.

20. Rodríguez-Fernández, V., Gonzalez-Pardo, A., & Camacho, D. Finding behavioral patterns of UAV operators using multichannel hidden Markov models. *IEEE Symposium Series on Computational Intelligence (SSCI)*, Athens, Greece, 2016, IEEE, pp. 1-8. DOI: 10.1109/SSCI.2016.7850101.

21. Abakumov, A., Kharchenko, V., & Ponochovnyi, Y. UAV Cyber Resilience Assessment Method: Combining IMECA, Penetration Testing and State-space Markov Modeling. *International Journal of Computing*, 2025, vol. 24, iss. 4, pp. 790-801. DOI: 10.47839/ijc.24.4.4346.

22. Kharchenko, V., Kliushnikov, I., Rucinski, A., Fesenko, H., & Illiashenko, O. UAV Fleet as a Dependable Service for Smart Cities: Model-Based Assessment and Application. *Smart Cities*, 2022, vol. 5, iss. 3, pp. 1151-1178. DOI: 10.3390/smartcities5030058.

23. Kabashkin, I., Iskakov, D., Topilskiy, R., Tlepiyeva, G., Sultanov, T., & Sansyzbayeva, Z. Communication Infrastructure Design for Reliable UAV Operations in Air Mobility Corridors. *Drones*, 2025, vol. 9, iss. 6, article no. 401. DOI:10.3390/drones9060401.

24. Kliushnikov, I. Safety and security assessment of unmanned aerial vehicles application using Markov models. *Systemy ozbroiennia i viiskova tekhnika – Systems of Arms and Military Equipment*, 2023, no. 4(76), pp. 51-57. DOI: 10.30748/soivt.2023.76.05. (In Ukrainian).

25. Kharchenko, V., Ponochovnyi, Y., Ivanchenko, O., Fesenko, H., & Illiashenko, O. Combining Markov and Semi-Markov Modelling for Assessing Availability and Cybersecurity of Cloud and IoT Systems. *Cryptography*, 2022, vol. 6, iss. 3, article no. 44. DOI: 10.3390/cryptography6030044.

Received 14.08.2025, Received in revised form 10.09.2025
Accepted date 03.11.2026, Published date 08.12.2025

ISSN 1814-4225 (print)
ISSN 2663-2012 (online)

МАРКОВСЬКЕ МОДЕЛЮВАННЯ ЛЮДИНО-МАШИННОЇ ВЗАЄМОДІЇ В AR-СЕРЕДОВИЩІ ДЛЯ СИСТЕМ МОНІТОРИНГУ НЕБЕЗПЕЧНИХ ТЕРИТОРІЙ НА ОСНОВІ UAV/UGV

Є. О. Канарський, В. С. Харченко, О. О. Орєхов, Ю. Л. Поночовний

Предметом дослідження є марковські процеси, що використовуються для формального опису динаміки станів безпілотних апаратів, керованих оператором за допомогою людино-машинних інтерфейсів на основі доповненої реальності. В межах дослідження безпілотні літальні та наземні апарати розглядаються як складні багатостанові технічні системи, функціонування яких визначається як технічними характеристиками, так і особливостями взаємодії людини з інтерфейсом керування. **Метою** дослідження є оцінювання впливу інтерфейсів людино-машинної взаємодії на основі доповненої реальності на безпомилковість прийняття рішень оператором безпілотних систем, а також на його реактивність у процесі керування та реагування на зміну станів системи. **Завданнями** даного дослідження є розробити марковські моделі (a) без урахування відмов і помилок оператора безпілотних систем, з повним відновленням; (b) без урахування відмов з можливістю допущення помилок оператором, з повним відновленням; (c) з урахуванням відмов без помилок оператора безпілотних систем, з повним відновленням; (d) з урахуванням відмов і помилок оператора, з повним відновленням; (e) без урахування відмов з можливістю допущення помилок оператором, з наявною резервною безпілотною системою. Отримані ланцюги Маркова мають бути використані для моделювання і подальшого порівняння впливу різних умов на систему. В **результаті** дослідження було отримано (a) класифікатор станів безпілотних літальних апаратів в складі системи моніторингу небезпечних середовищ на основі можливої наявності відмов, помилок оператора та резерву апаратів; (b) моделі Маркова для різних сценаріїв роботи системи; (c) результати симуляції роботи системи на основі розроблених моделей Маркова. **Висновок**. Наукова новизна полягає у наступному: вперше запропононвано метод оцінювання готовності систем моніторингу з інтерфейсами людино-машинної взаємодії на основі доповненої реальності, що базується на одно та багатофрагментних марковських моделях, які враховують дії оператора, часткові відмови та наявність резервних безпілотних апаратів. Метод кількісно оцінює вплив доповненої реальності не тільки на суб'єктивні показники, але й на показники готовності та надійності системи в цілому.

Ключові слова: доповнена реальність; безпілотні системи; ланцюги Маркова; людино-машинна взаємодія.

Канарський Євгеній Олександрович – асп. каф. кібербезпеки та інтелектуальних інформаційних технологій, Національний аерокосмічний університет «Харківський авіаційний інститут», Харків, Україна.

Харченко Вячеслав Сергійович – член-кореспондент НАН України, д-р техн. наук, проф., зав. каф. кібербезпеки та інтелектуальних інформаційних технологій, Національний аерокосмічний університет «Харківський авіаційний інститут», Харків, Україна.

Орєхов Олександр Олександрович – канд. техн. наук, доц., проф. каф. кібербезпеки та інтелектуальних інформаційних технологій, Національний аерокосмічний університет «Харківський авіаційний інститут», Харків, Україна.

Поночовний Юрій Леонідович – д-р техн. наук, проф., проф. каф. інформаційних систем та технологій, Полтавський державний аграрний університет, Полтава, Україна.

Yevhenii Kanarskyi – PhD Student, National Aerospace University “Kharkiv Aviation Institute”, Kharkiv, Ukraine,
e-mail: y.kanarskiy@csn.khai.edu, ORCID: 0000-0001-9066-8642.

Vyacheslav Kharchenko – Corresponding Member of National Academy of Science of Ukraine, DrS, Professor, Head of Department, National Aerospace University “Kharkiv Aviation Institute”, Kharkiv, Ukraine,
e-mail: v.kharchenko@csn.khai.edu, ORCID: 0000-0001-5352-077X, Scopus Author ID: 22034616000.

Oleksandr Orekhov – PhD, Professor, National Aerospace University “Kharkiv Aviation Institute”, Kharkiv, Ukraine,
e-mail: a.orehov@csn.khai.edu, ORCID: 0000-0001-6957-1934, Scopus Author ID: 55347351300.

Yuriy Ponochovnyi – DrS, Professor, Poltava State Agrarian University, Poltava, Ukraine,
e-mail: yuriy.ponochovnyy@pdau.edu.ua, ORCID: 0000-0002-6856-2013, Scopus Author ID: 56446990700.